COMPUTATIONAL STUDY OF AIR FLOW INTERACTIONS AND DRAG REDUCTION TECHNIQUES IN SIMPLIFIED PASSENGER VEHICLE

[1]Mitali Mangesh Jadhav, [2]Suhani Sanjay Patel, [3]Dhruvin V Shah, [4]Arpit N Patel

[1,2]Aeronautical Engineering Department SVIT, Vasad, Gujarat, India

[3,4]Assistant Professor Aeronautical Engineering Department, SVIT, Vasad Gujarat, India

[1]mitalimjadhav29@gmail.com,[2]patelsuhani@gmail.com,[3]dhruvinshah.aero@svitvasad.ac.in,[4]arpitpatel.aero@svitvasad.ac.in

Abstract—**Aerodynamic characteristics of passenger cars have been a fruitful area of research for several years, and continue to this day. The Ahmed body represents simplified geometry of generic passenger car that can be used to study the flow characteristic of vehicles. The main objective of this paper is to understand the aerodynamic characteristics and drag reduction techniques of an isolated passenger car. To study this problem, Ahmed car model with different rear slant angles (0°- 40°), is simulated at the air velocity of 35 m/s using CFD. Also the effect of Reynolds Number, Ground clearance and rear end drag reduction techniques (varying fore body rounding and boat-tailing) on drag coefficient is identified. The computational part includes numerical simulation of the flow around the Ahmed car body employing CFD (Computational Fluid Dynamics) techniques. The designing of model and CFD simulation is carried out in FLUENT (ANSYS 15.0). Major findings show that the rear part of the vehicle plays a major role in formation of wake. Significant drag reduction was observed for 25° rear slant angle resulting from the reduced recirculation region behind the model.**

Index Terms— **Ahmed car body, CFD, k-Epsilon model, Drag Coefficient, critical rear slant angle.**

I. INTRODUCTION

As the human population increases in number, the need for more practical and efficient methods of transportation becomes more vital. In the past, simply constructing more roads and highways to cope with the growing number of vehicles has solved this problem to some extent. Obviously this trend cannot continue indefinitely, so a method that is currently being considered by several organizations is the Automated Highway System (AHS) i.e. The vehicles are grouped in platoons.

As in [10] heavy duty vehicles use a lot of fuel. For a heavy duty vehicle driving at highway speeds, more than 40% of the fuel consumption is caused by the aerodynamic drag. In order to reduce the fuel consumption of heavy duty vehicles, the aerodynamic drag needs to be reduced.

II. TECHNICAL BACKGROUND

A. Blunt Body Aerodynamics

As in [1], a bluff or blunt body is a body where most of the drag is pressure drag. "Fig. 1,"shows that the pressure drag is contributing the most to the total drag for bluff bodies. The high contribution of pressure drag is caused by the large surfaces in the direction of the flow
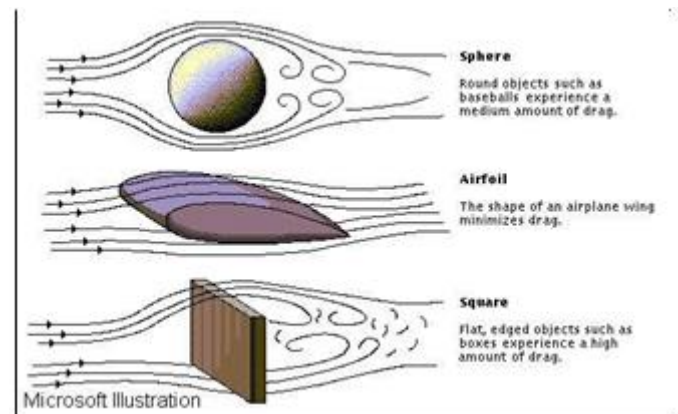

Fig. 1.   Pressure drag for various shapes.

B.   Ahmed Car body

"Fig. 2," shows the geometry of a simplified model known as Ahmed body which generates characteristics similar to a real vehicle flow field neglecting the effects of wheels, engine and projected surfaces like mirrors. The Ahmed body is made up with very simple geometry, consist of a round front part, a moveable rear slant part of the body to study the coefficient of drag and flow separation phenomena at different slant angles, and a rectangular box(at middle), which connects the front part and the rear slant part. This is one of the most suitable and simplest bluff bodies for analysis which consider the minimum requirement of actual road vehicle. The chosen model generates: a strong two-dimensional flow in front, a relatively uniform flow in the middle, and a large structured wake at the rear.
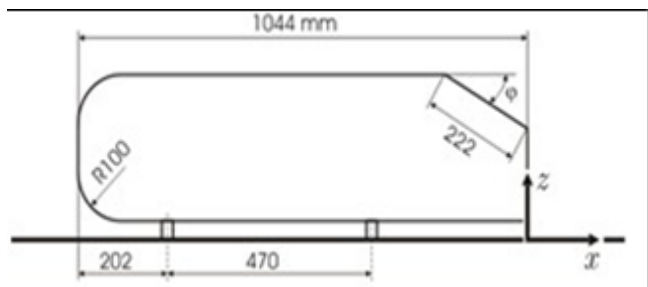
Fig. 2.   Ahmed body (Dimensions in mm).

C.   Rear Drag Reduction Techniques

The main aim of using rear drag reduction technique is to reduce the drag caused by the flow separation. The pressure difference between the front and the rear part of the Ahmed car body creates a force in the downwind direction, so it is important to increase the pressure at the back of the vehicle to reduce this pressure difference and hence the drag. To reduce the drag, some rear drag reduction techniques are used such as Boat-Tailing as shown in "Fig. 3," and Fore-Body Rounding as shown in "Fig. 4,".
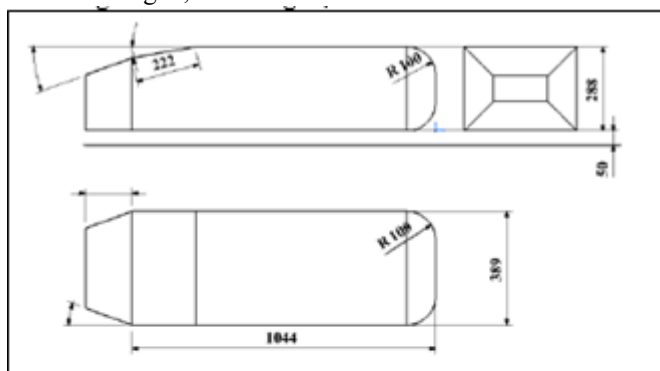

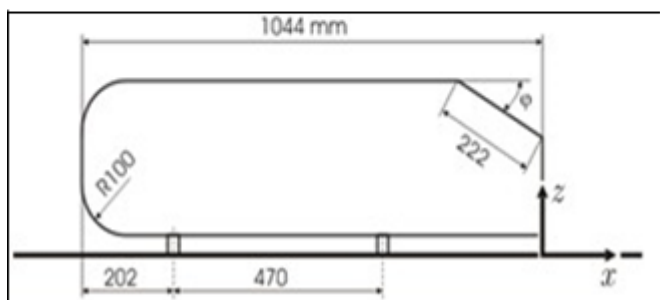Fig. 3.   Boat-Tailing (Rear-End Drag ReductionDevice)

Fig. 4.   Fore-Body Rounding (Rear-End Drag Reduction Device)

III. LITERATURE REVIEW

[2] Ahmed analyzed time averaged wake structure around the Ahmed body at a Reynolds number equal to 1.2*106 by varying the rear slant angle from 0-40°in increments of 5°. The main aim was to study the time average flow structures present in the wake of basic vehicle type body and   analyze

the effect of geometry on wake structure, pressure distribution and drag. Results revealed that almost 85% of body drag is pressure drag.

[5] T. Han (1992) applied three dimensional Navier Stokes analysis to optimize the rear-end shape of a vehicle-like body in ground proximity. Aerodynamic shape optimization was performed on Ahmed body with three shape parameters: backlight angle (0º to 30º), boat tail angle (0º to 30º) and ramp angle (0º to 20º). The optimum design geometry (17.8° backlight, 18.9° boat tail and 9.2° ramp) was obtained after 15 Navier-Stokes analyses. The experimentally determined optimum shape, for similar body, fell in the range of 15-18° back light, 15-22° boat tail and 9-14° ramp. The measured drag coefficient reduction was 0.13.

[6] Bayraktar et al. examined the aerodynamics of Ahmed reference body with full scale wind tunnel experiments and by solving the time dependent, three dimensional, Reynolds-averaged Navier Stokes equations. The main concern was to observe the effect on the lift and drag coefficients due to variation of rear slant angles (0, 12.5, and 25 degrees) and Reynolds number (2.2*106to 13.2*106) and calculating wind-averaged drag coefficients. The results from experimental and computational methods were presented and compared with each other.

[11] Gokul Krishnan Rajamani (2006) investigated time-averaged characteristics of a simplified, generic passenger vehicle, called the Ahmed car model computationally. Three different platoon combinations were analyzed which includes a two, three and six model platoons for various rear end configurations of the Ahmed model geometry. Experiments were conducted in RMIT University Industrial Wind Tunnel for analyzing the effects of drafting on drag coefficients using two different scales of Ahmed car models. The critical rear slant angle was found to be 25° from the 2D analysis and 30° from 3D analysis. At extremely close proximity, the models experienced more pressure recovery at their rear end, which reduced the drag coefficient. Surprisingly, at some of the close vehicle spacing, the drag coefficients reached values that were higher than that of a vehicle in isolation.

[14]S.P. Doppenberg (2015) investigated the drag reduction in platoon of trucks equipped with rear drag reduction devices to reduce the fuel consumption of the platoon and its individual components. This research was performed with basic models of trucks in a platoon using CFD. Different simulations were done where the spacing between trucks was varied, as well as the tail plate angle and the body front rounding. He concluded that at short spacing the best way was to equip only the last body with a tail so the streamlines could follow the contours of the platoon and the wake was reduced by the tail on the last body. The biggest drag reduction was of 124 drag count which was achieved with   a 12° tail. Varying the front rounding of all vehicles in the platoon lead to an optimal radius where the

drag decrease due to the rounding and the pressure increase at the back of the trucks due to the platooning. It showed that a rounding radius of 36*mm*for a scaled model was the best case.

IV. MODELLING AND ANALYSIS

In ANSYS 15 Design Modeler, Ahmed car body having dimensions as follows: 1044mm long, 327mm wide and 288mm is created. "Fig. 5," shows a high single body domain of air which is created surrounding the Ahmed body. The locations of the inlet and outlet are placed far enough so that the flow is fully developed before it reaches the model and also the wake flow can be recorded completely once the flow leaves the model.

Fig. 5. Single air body domain

A. Meshing Details

The model is kept 50 mm above the ground. "Fig. 6,"shows the generated mesh. The Ahmed car model is surrounded by a very fine tetrahedral grid, since this area is extremely important for recording flow structures. Inflation layers are created along the walls of the Ahmed model to accurately capture the flow separations from its rear.
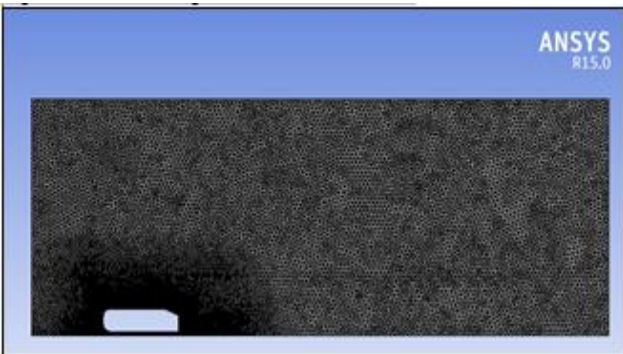

Fig. 6. Meshing around Ahmed body

B. Boundary Conditions:

Standard k-epsilon model with Inlet velocity V = 35m/s is used. Density of air is 1.225 kg/m3, temperature is 288.16 K and viscosity is 1.7894e-05 kg/m4. Boundary conditions are - uniform velocity at inlet, uniform pressure at outlet, symmetry at wall. Solution method is pressure-velocity coupling scheme: least square cell based method, pressure as linear and setting the momentum, turbulence kinetic energy, turbulence dissipation rate as second order upwind for the 1000 iterations. Further, in solution controls momentum is taken as 0.7, pressure as 0.3 and turbulence viscosity factor as 0.8 for all 1000 iterations.

C. Grid Independency Test

The grid independency test is performed for isolated 25° rear slant configuration of 2D Ahmed model. "Fig. 7" shows variation of drag coefficient with grid size. It indicates that a grid size of approximately 40,000 cells provides sufficient accuracy and it is adopted as standard for all future working grids when models are analyzed in isolation.
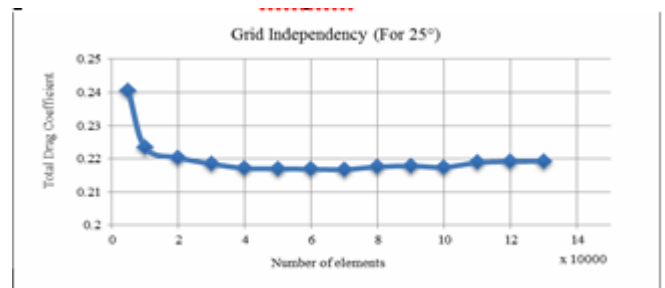

Fig. 7. Grid Independency Test.

V. RESULTS AND DISCUSSION

A. Critical Rear Slant Angle

The drag coefficients are calculated for 10 different rear slant angle of the Ahmed body ranging from 0 to 40 degree. "Fig. 8" shows rear slant angle vs. Cd graph. The graph indicates that minimum drag is obtained for rear slant angle, φ= 25 degree.
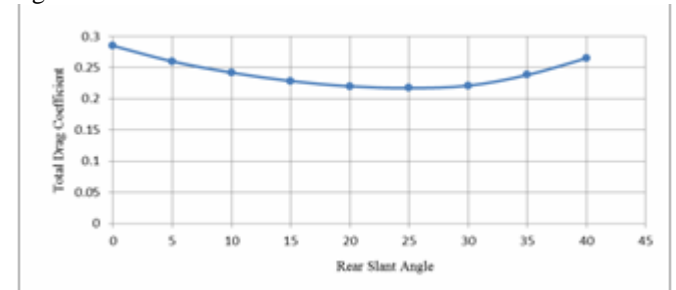

Fig. 8. Rear slant angle vs. Cd graph

It is observed that the drag coefficient decreases as rear slant angle is increased from 0° up to 25°, where it reaches the minimum value of 0.21716 and then continually goes on increasing till 40°. "Fig. 9" to "Fig. 15" shows Velocity contours which give the velocity distribution along different geometric sections of the Ahmed body. The green colored region corresponds to the velocity of 35 m/sec, while blue area depicts low velocity and red area shows high velocity region.

"Fig. 9" shows that for 0° rear slant angle the flow after reaching the front part stays attached on the body and separates at the sharp rear end leaving a large recirculation region behind the base. This resulted in the increase of base pressure drop which constitutes the main reason for its highest drag coefficient among various rear slant configurations.
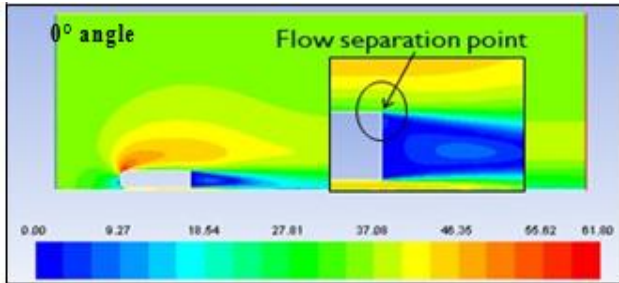

Fig. 9. Velocity Contour of 0° rear slant angle.

"Fig. 10" shows that 5° rear slant configuration exhibits more similar flow characteristics to that of the 0° rear slant configuration, except for the reduction of drag coefficient. This reduction in drag coefficients is mainly due to the reduced recirculation region.
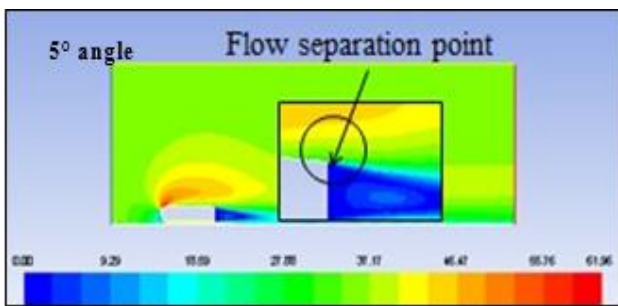

Fig. 10. Velocity Contour of 5° rear slant angle.

"Fig. 11" shows that 15° rear slant configuration, exhibits a considerable reduction in the size of the recirculation region. Hence the pressure recovery at the base is improved, thus it results in the reduction of drag coefficient.
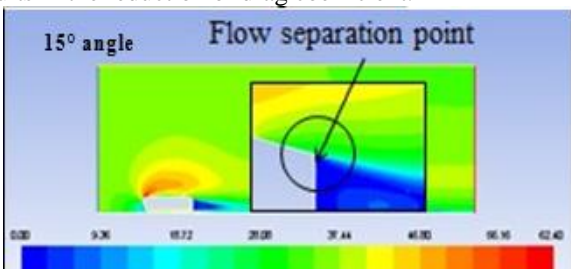

Fig. 11. Velocity Contour of 15 ° rear slant angle.

"Fig. 12" shows the 25° rear slant configuration exhibits the least drag coefficient of all the rear slant configurations of 2D-Ahmed model geometry. The recirculation region is considerably reduced. The recirculation region is decreased since the rear slant support to have the flow attached to it. Also,

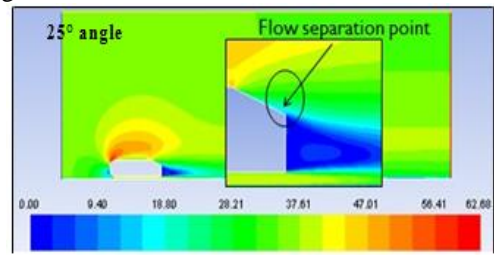this effect resulted in the decrease of pressure drop and low drag coefficients.

Fig. 12. Velocity Contour of 25° rear slant angle.

An increase of angle contributed to the increase of drag coefficient which is observed for the 30˚, 35˚ and 40˚ rear slant configurations. "Fig. 13" shows that at 30˚ rear slant angle, the drag coefficient increased as now the separation point started to shift towards the leading edge of the rear slant angle. "Fig. 14" shows that for 35 degree slant angle, separation point further shifts upstream and "Fig. 15" shows the for 40 degree, separation point reaches the leading edge of the rear slant angle resulting in maximum drag as shown in figure. The recirculation region is increased since the rear slant does not support to have the flow attached to it. Also, this effect resulted in the increase of pressure drop and high drag coefficient.
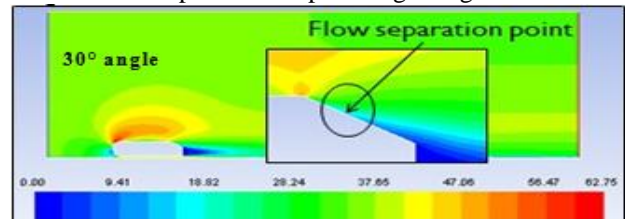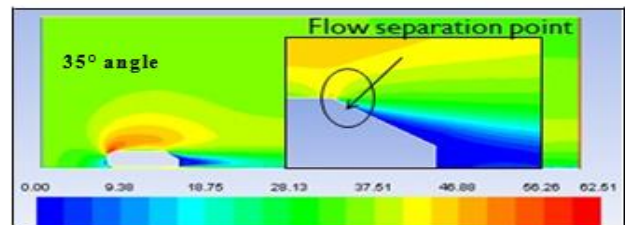

Fig. 13. Velocity Contour of 30° rear slant angle

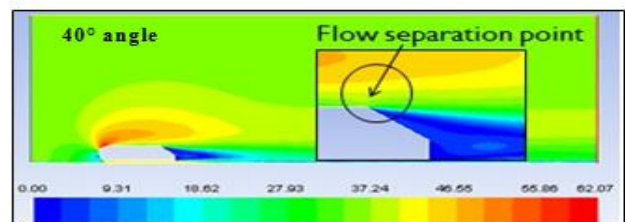Fig. 14. Velocity Contour of 35° rear slant angle

Fig. 15. Velocity Contour of 40° rear slant angle

B. Effect of Reynolds Number

"Fig. 16" shows Reynolds Number vs. Cd graph. The graph indicates that drag coefficient slightly decreases as the Reynolds number increases.
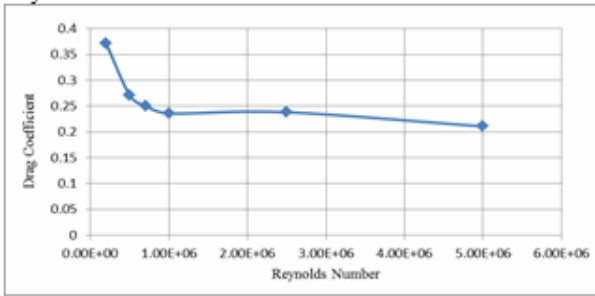
Fig. 16. Reynolds Number vs. Cd graph.

C. Effect of varying fore body

For having a better understanding of drag coefficient on Ahmed body, the body with different front nose radius is designed and analyzed at 25° rear slant angle by keeping all other parameters such as ground clearance, length, velocity same. The results obtained after successful simulation of Ahmed body for different nose radius at 25° slant angle, suggest that there is reduction in drag as the nose radius increases.

"Fig. 17" shows the graph for different nose radius at 25° slant angle. It is observed that with the increase in nose radius from 0 to 0.1 m, there is a reduction in coefficient of drag which ultimately reduces fuel consumption.
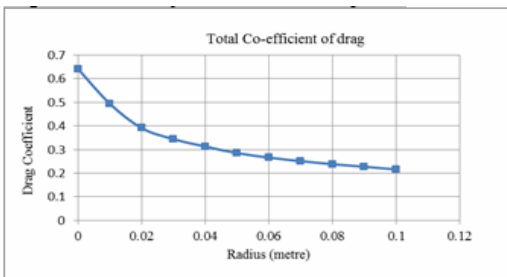

Fig. 17. Front nose radius vs. Cd graph.

"Fig. 18" shows that when nose radius is low at the front part then it acts like a sharp edge so the flow at the front starts to separate from this edge, which results in increase in drag. "Fig. 19" and "Fig. 20" shows that with increase in nose radius, it forms an edge with fillet so the flow does not separate suddenly at front part. However after reaching rear part there is flow separation.
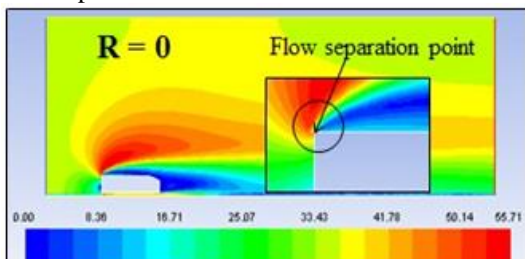

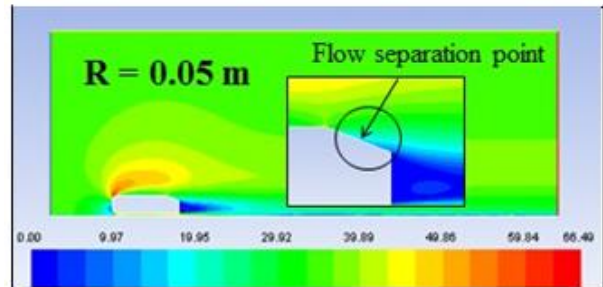Fig. 18. Velocity Contour for no front rounding at 25° rear slant angle.

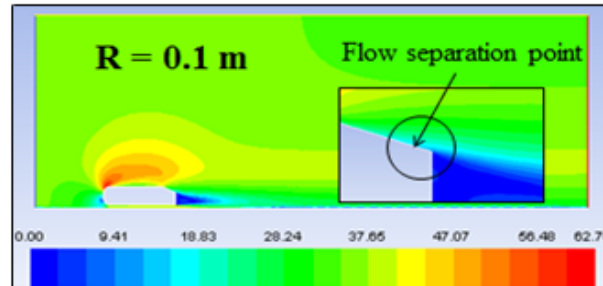Fig. 19. Velocity Contour for front rounding of 0.05m at 25° rear slant angle.

Fig. 20. Velocity Contour for front rounding of 0.1 m at 25° rear slant angle.

D. Effect of Boat-tailing

For proper understanding of drag coefficient on Ahmed body another drag reduction technique is employed i.e. boat-tailing. By tapering the rear end of a vehicle, we tend to increase base pressure by providing pressure recovery of the surrounding flow before it leaves the sharp back edges and forms a wake. The idea is to trap a vortex or eddy in the corner between the rear of the trailer and boat-tail plates. The eddy turn the flow inwards as it separates from the rear of the trailer and creates a virtual boat-tail and thus increase the base pressure acting on the rear of the vehicle and reduce the net aerodynamic drag of the vehicle. This increased base pressure provides a lowered overall pressure difference from front-to-back of the vehicle. "Fig. 21" shows Boat tail length vs. Cd graph for various boat tail angles at 25° rear slant angle.
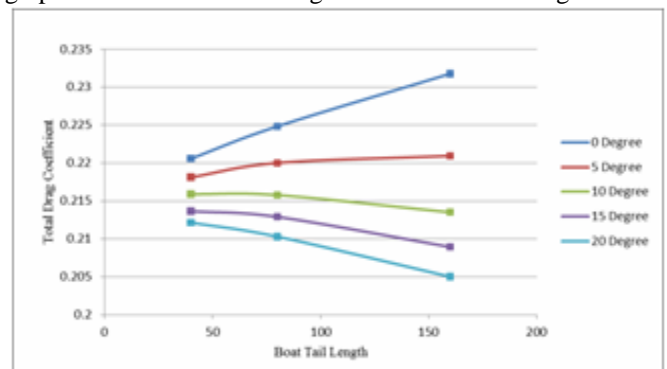

Fig. 21. Boat-tail length vs. Cd graph for different boat tail angles.

✓ From the analysis of varying the boat tail angle and length on Ahmed car model, the results can be interpreted in the following manner.

✓ For the cases of boat tail angle of 0 and 5 degree, by varying length of boat tail (40, 80,160) drag coefficient increases. This can be because the angle is small enough to contribute towards drag reduction. As we know that the magnitude of the drag generated by an object depends on the shape of the object, increase in boat tail length increases the area and hence the drag.

✓ For boat tail angles 10, 15, 20 degree, there is reduction of drag on increasing boat tail length.

E. Effect of Ground clearance

In order to achieve a better body design with reference to ground clearance the simulation is done by changing the ground clearance from 0.01m to 0.05m. "Fig. 22" shows simulation result for Ahmed body i.e. variation of coefficient of drag with ground clearance.
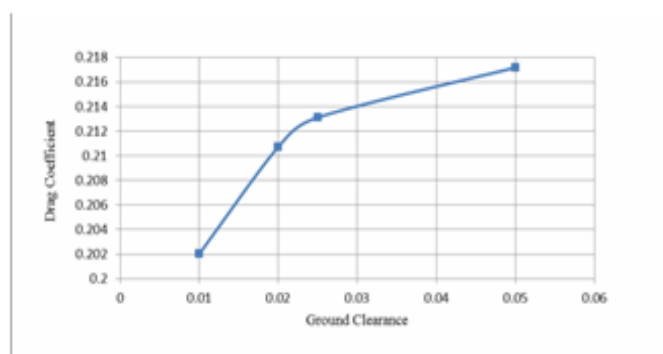

Fig. 22. Ground Clearance vs. Cd graph for 25° rear slant angle

With the increase in ground clearance, there is formation of eddies in underside flow which increases the drag coefficient.

CONCLUSION

In the present work, the simulation of Ahmed body is carried out for different rear slant angle, Reynolds Number, nose radius, boat-tailing along with variation in ground clearance.

It has been found that the drag coefficient decreases as rear slant angle is increased from 0° up to 25°, where it reaches the minimum value and then continuously goes on increasing till 40°. Also, it has been found that there is reduction in drag as the Reynolds Number and nose radius increases. On increasing boat tail length it was noted that for small boat tail angles (i.e. 0-5°) the drag coefficients increased whereas for relatively large boat tail angles (i.e. 10°-20°) a decrement in drag coefficients was observed. Increasing the ground clearance has a counter effect on coefficient of drag.

REFERENCES

[1] "Fundamentals of Aerodynamics", 5th edition, John D. Anderson, McGraw-Hill Book Co.

[2] Ahmed, S.R., Ramm, G., Faitin, G., "Some Salient Features of the Time Averaged Ground Vehicle Wake.". Society of Automotive Engineers, Inc., Warrendale, PA. (SAE-TP-840300) 1984

[3] K. R. Cooper, The effect of front-edge rounding and rear-edge shaping on the aerodynamic drag of bluff vehicles in ground proximity, Report 0148-7191 (SAE Technical Paper, 1985)

[4] W. H. Hucho and S. R. Ahmed, "Aerodynamics of Road Vehicles" (Butterworth's, London, 1987)

[5] T. Han, D. C. Hammond, C. J. Sagi "Optimization of bluff body for minimum Drag in ground proximity", AIAA Journal, Vol. 30, No. 4 (1992), pp. 882-889

[6] I. Bayraktar, D. Landman, and O. Baysal "Experimental and Computational Investigation of Ahmed Body for Ground Vehicle Aerodynamics", SAE Technical Paper 2001-01-2742, 2001, doi: 10.4271/2001-01-2742.

[7] Lienhart, H. and Becker, S., "Flow and Turbulence Structure in the Wake of a Simplified Car Model," SAE Technical Paper 2003-01- 0656, 2003, doi: 10.4271/2003-01-0656.

[8] R. M. Wood and S. X. Bauer, "Simple and low-cost aerodynamic drag reduction devices for tractor trailer trucks", Report (SAE Technical Paper No. 2003-01-3377, 2003).

[9] R. M. Wood "Impact of advanced aerodynamic technology on transportation energy consumption", Report (SAE Technical Paper No. 2004-01-1306, 2004).

[10] G. Vino, S. Watkins, P. Mousley, J. Watmuff, S. Prasad, "Flow structures in the near-wake of the Ahmed model", Journal of Fluids and Structures 20 (2005) 673–695

[11] Gokul Krishnan Rajamani, "CFD Analysis of Air Flow Interactions in Vehicle Platoons", School of Aerospace, Mechanical and Manufacturing Engineering, RMIT University, August 2006.

[12] Ivan Korkischko & Julio Romano Meneghini "Experimental investigation and numerical simulation of the flow around an automotive model: Ahmed body", 19th International Congress of Mechanical Engineering, November 5-9, 2007, Brasília, DF.

[13] A. Lahayea, A. Leroya & A. Kourtaa "Characterization of a square back Ahmed body near wake flow", 21`eme Congress Francis de M´ecanique. (2013)

[14] S.P. Doppenberg "Drag Influence of Tails in a Platoon of Bluff Bodies",Delft University of Technology, 2015

Andrew Watts "Computational Characterization of Drag Reduction for Platooning Heavy Vehicles", Auburn, Alabama, May 10, 2015.